SEISMIC RESPONSE OF MULTISTORY FRAMES CLAD WITH CORRUGATED PANELS

H.K. Ha and F. Hassan

SYNOPSIS

Cold-formed corrugated steel panels are effective for controlling the drift of multistory frames provided that the cladding is properly connected to the bare frame. This paper presents a method of analysis of the cladding itself and of the integrated frame. The cladding stiffness matrix is derived taking into account the flexibility of the connections, shear strains in the sheeting, bending of the corrugation profile, and axial strains in the perimeter members. Analyses of two welded shear diaphragms yield results comparable to those of finite element analyses and tests.

The conventional direct stiffness technique is then used to evaluate the seismic response of two clad frames having 26 and 40 stories with 3 bays. The results obtained are cast in generalized forms applicable to other similar frames. The use of cladding does reduce the lateral deflections but may increase the member forces, especially the axial forces in the adjacent columns. It is recommended that overstiff cladding be avoided until further studies on the energy dissipation capacity and overall ductility of cladding indicate otherwise.

RESUME

Les revêtements en tôles ondulées formées à froid sont efficaces pour contrôler les déplacements latéraux des cadres multi-étagés pourvu que ces revêtements soient bien attachés aux cadres. Cet article contient une méthode d'analyse du revêtement lui-même et du cadre renforcé. On a dérivé la matrice de rigidité du revêtement en tenant compte de la flexibilité des attaches, du cisaillement et de la flexion dans les tôles et des déformations axiales dans les membrures périphériques. L'analyse de deux diaphragmes en tôles ondulées soudées a donné des résultats semblables à ceux obtenus par éléments finis et expérimentalement.

On a utilisé la méthode de rigidité classique pour déterminer la réponse aux séismes de deux cadres de trois travées, l'un ayant 26 niveaux et l'autre 40 niveaux, renforcés tous les deux par des revêtements. Les résultats sont présentés sous une forme générale de façon à ce qu'ils puissent être utilisés pour d'autres cadres similaires. On a constaté que les revêtements servant de remplissage réduisent les déplacements latéraux mais ils peuvent augmenter les efforts dans les membrures surtout les efforts axiaux dans les poteaux adjacents. En conséquence on recommande de ne pas utiliser des revêtements très rigides jusqu'à ce que d'autres études sur la capacité d'absorption d'énergie et sur la ductilité de ces revêtements démontrent qu'il est possible de les utiliser.

H.Kinh Ha obtained his D. Eng. from Concordia University in 1972. He is currently Associate Professor of Engineering in the Centre for Building Studies of Concordia University, Montreal, Quebec.

F.Hassan obtained his M.Eng. from Concordia University in 1978. He is currently a Research Assistant and a doctoral student in the Centre for Building Studies of Concordia University.

INTRODUCTION

Cold-formed corrugated steel panels possess substantial resistance against in-plane shear forces; but despite their increased use as cladding or partitions in multistory buildings, designers tend to ignore the panels' contribution to the overall stiffness of the structure. This situation may be attributed to the lack of understanding of the behaviour of the component cladding and the difficulty in integrating its stiffness with that of the bare frame. By taking into consideration the stiffening effect of the in-filled panels, the true behaviour of the system can be evaluated and that may result in significant reduction in the overall cost of the structure. To realize fully their advantages, the panels would have to be considered as "permanent" structural members and designed to meet the structural requirements. The panel size, its profile and the connections should be able to develop: (i) the required shear stiffness and strength; and (ii) sufficient bending stiffness to carry the transverse loads and to prevent premature shear buckling.

Extensive research programs have been carried out to study the linear, static behaviour of corrugated shear diaphragms. Of particular significance are the works of the Cornell Group and of Bryan and co-workers; the former led to the development of AISI's design manual (1) for steel diaphragms and the latter to the adoption of the European Recommendations for the Stressed Skin Design of Steel Structures (2). Other researchers have also made significant contribution to the understanding and utilization of cold-formed steel cladding (3). With regard to the integrated behaviour of multistory clad frames, much less research activity has taken place. Analysis methods based on finite element idealization of the panels have been used by Miller (4,5) and Oppenheim (6,7). In these studies, the 12 by 12 stiffness matrix of a shear diaphragm is obtained by static condensation of the overall diaphragm stiffness matrix. Results of linear dynamic analysis indi-

cated that significant reduction in the lateral deflection can be obtained with the use of cladding (5). In Oppenheim's work (7) the dynamic behaviour of clad frames subjected to various sinusoidal ground motion was investigated. The frame was modelled with elasto-plastic girders and with panels failing in a brittle manner at a certain relative drift. It was found that because of the whipping effect, panels in the upper stories may fail prematurely.

Other techniques of analysis have also been used. Bryan and Davies' method (8) utilizes fictitious bracing members to represent the cladding. The method proposed by El-Dakhakhni (9) is based on the superposition of the applied lateral forces with the cladding restraining forces to achieve compatibility of the story drifts. These last two methods are much simpler to use than the finite element method; however, they fail to account properly for the interaction between the story drifts and the column axial deformations. In addition, these methods presuppose the knowledge of the cladding stiffnesses. In all of the above studies, little information on the effects of the cladding upon the internal member forces has been given.

This paper presents an integrated approach to the analysis of multi-story clad buildings. In this approach the cladding is explicitely modelled as an integral part of the overall structure, and thus the cladding stiffness need not be determined in advance. The method has most of the advantages offered by the finite element method; it is, however, simpler to use and more efficient in terms of computer storage and computation. The analysis is based on the direct stiffness technique and composed of three main phases: (i) development of a 4 by 4 stiffness matrix for each cladding fitting into one story one bay of the building frame; (ii) generation of the assembled stiffness matrix for the overall structure; and (iii) solutions by mode superposition for the displacements, and internal forces in the components including those of the cladding fasteners. In the following, only phase (i) is described in detail as the others are part of the standard stiffness approach. Behaviour of the overall structures will be discussed with reference to two specific clad multistory frames.

CLADDING STIFFNESS MATRIX

The Structural System

A typical steel diaphragm (Fig. 1) comprises several corrugated steel sheets, or panels fastened to one another along the laps and to the four perimeter members. The connections may be made by mechanical fasteners or by welding. Welded connections would result in a much stiffer and

stronger diaphragm. The direction of corrugations is arbitrary; however, since the story height is usually less than the bay width, corrugation generator running in the vertical direction would yield higher out-of-plane bending stiffness. The perimeter members are pin-connected to each other such that they promote a pure shear state in the sheeting. Similarly, the assembled diaphragm is in turn pin-connected to the framing girders and columns at the four corners. Details of the connections between the diaphragm corners and the upper girder should be designed so as to minimize the transfer of vertical forces between the two components, and at the same time to permit the full transmission of lateral forces. Several such connection details have been suggested in Ref. (4).

Assumed Deformation Patterns

Although the theory presented here can readily be extended to the nonlinear dynamic behaviour of clad frames, the present development deals only with the structural behaviour at service loads where all components are assumed to be linear elastic. Under the action of a load applied horizontally at the diaphragm corner (Fig. 2), the perimeter frame is rotated by an angle as shown. The diaphragm deflection r, corresponding to the load P, is due to several factors: (i) flexibility of the connections; (ii) shear strains in the sheeting; (iii) distortion of the profile; and (iv) axial strains in the vertical perimeter members. The strain energy associated with each of these deformation modes can be determined in terms of the overall shear deflection r, and the displacements of the panels. Consider a typical panel k of the diaphragm (Fig. 3): its new position may be specified by 3 rigid body movements u^k, v^k, θ^k and a shear deformation γ^k. For convenience, these movements are arbitrarily associated with the lower left corner of the panel. Thus, the total number of degrees of freedom of the diaphragm is one more than four times the number of panels.

The total potential energy of the diaphragm is, symbolically

$$\Pi = U - P.r = \tfrac{1}{2}\{D\}^T[S]\{D\} - P.r \qquad (1)$$

in which U = the total strain energy; {D} = the vector of diaphragm degrees of freedom, i.e.,

$$\{D\}^T \quad \langle r,\ u^1,\ v^1,\ \theta^1,\ \gamma^1,\ \ldots,\ u^n,\ v^n,\ \theta^n,\ \gamma^n \rangle \qquad (2)$$

n = number of panels; and [S] = the diaphragm generalized stiffness matrix to be derived. Minimizing the total potential energy with respect to the generalized displacements {D} leads to the diaphragm stiffness equation:

$$[S]\{D\} = \{P\} \tag{3}$$

in which $\{P\}$ contains only one non-zero element, P, at the first location corresponding to the degree of freedom r. Equation (1) shows that the stiffness matrix $[S]$ may be derived by forming the strain energy expression in terms of the degrees of freedom $\{D\}$.

Let i be a point in a panel k and located at the coordinates (x_i, y_i) with respect to the panel origin. The x- and y-displacements of this point are, respectively: (Fig. 3)

$$u_i = u^k - \theta^k y_i + \gamma^k y_i \tag{4}$$

$$v_i = v^k + \theta^k x_i \tag{5}$$

Similarly, if j is a point on a perimeter member and located at a vertical distance y_j with respect to the diaphragm origin (lower left corner of the diaphragm), its displacements are: (Fig. 2)

$$u_j = y_j \frac{r}{b} \tag{6}$$

$$v_j = 0; \tag{7}$$

in which b = depth of the diaphragm (in vertical direction). In the development that follows, it is assumed that the direction of the corrugation generator is vertical.

Strain energy in seam connections -- A seam connection between two panels, k and k+1, may be idealized as a spring with the end i attached to panel k and the end i' attached to panel k+1. Using Eqs.(4) and (5), the displacements of i and i' can be evaluated, and the strain energy in this connection is written as

$$U_i = \tfrac{1}{2} s_i d_i^2 = \tfrac{1}{2}\{D_i\}^T[k_i]\{D_i\} \tag{8}$$

in which d_i = the spring deformation

$$d_i = [(u_i,-u_i)^2 + (v_i,-v_i)^2]^{\frac{1}{2}}; \tag{9}$$

$$\{D_i\}^T = \langle u^k \; v^k \; \theta^k \; \gamma^k \; u^{k+1} \; v^{k+1} \; \theta^{k+1} \; \gamma^{k+1} \rangle \tag{10}$$

$$[k_i] = s_i \begin{bmatrix} 1 & 0 & -y_i & y_i & -1 & 0 & y_i & -y_i \\ & 1 & w & 0 & 0 & -1 & 0 & 0 \\ & & y_i^2+w^2 & -y_i^2 & y_i & -w & -y_i^2 & y_i^2 \\ & & & y_i^2 & -y_i & 0 & y_i^2 & -y_i^2 \\ \text{Sym.} & & & & 1 & 0 & -y_i & y_i \\ & & & & & 1 & 0 & 0 \\ & & & & & & y_i^2 & -y_i^2 \\ & & & & & & & y_i^2 \end{bmatrix} \quad (11)$$

and w = width of the panel.

Strain energy in frame-to-panel connections -- The connecting spring is now considered to have end i attached to a panel k and the other end j attached to a perimeter framing member. The deformation in this connection is due to the differential movements of the connected components:

$$d_i^2 = (u_j-u_i)^2 + (v_j-v_i)^2 \quad (12)$$

Substituting Eqs.(4) to (7) into the above equation, the strain energy can be expressed in the form of Eq. (8) with matrices $\{D_i\}$ and $[k_i]$ defined as follows:

$$\{D_i\}^T = \langle r \; u^k \; v^k \; \theta^k \; \gamma^k \rangle \quad (13)$$

and

$$[k_i] = s_i \begin{bmatrix} \frac{y_j^2}{b^2} & -\frac{y_j}{b} & 0 & \frac{y_j y_i}{b} & -\frac{y_j y_i}{b} \\ & 1 & 0 & -y_i & y_i \\ & & 1 & x_i & 0 \\ \text{Sym.} & & & y_i^2+x_i^2 & -y_i^2 \\ & & & & y_i^2 \end{bmatrix} \quad (14)$$

Strain energy in the panel sheeting -- Consider now a panel k subjected to uniform shear stress

$$\tau = \frac{Q}{wt} \tag{15}$$

in which Q = the shear load on the panel; t = sheet thickness; and w = panel width. The strain energy in the panel k due to shear is

$$U_s^k = \frac{\tau^2}{2G} twb\alpha_1 = \frac{b\alpha_1}{2Gwt} Q^2 \tag{16}$$

in which G = shear modulus; and α_1 = ratio depending on the corrugation profile. For example, the factor α_1 for the open rectangular profile in Fig. 4 is

$$\alpha_1 = \frac{d+2h}{d} = (1 + 2\frac{h}{d}) \tag{17}$$

In addition to the shear strain in the sheeting, the shear load may also induce torsion and bending of the corrugation profile. Neglecting the relatively small effect of torsion, the strain energy in the panel due to profile bending can be approximately evaluated as: (for the rectangular profile of Fig. 4)

$$U_b^k = \frac{144h^3\ell^2}{2Et^3wbd} \alpha_2 Q^2 \tag{18}$$

in which

$$\alpha^2 = \frac{(d + 2h)(d^2 - 3\ell d + 3\ell^2)}{12hd^2} \tag{19}$$

For closed profiles, the factors α_1 and α_2 should be taken to be 1 and 0, respectively. Expressions similar to Eqs. (16) and (18) have been derived by Bryan and El-Dakhakhni (10). Ref.(11) gives a more refined version of Eq.(18).

The total strain energy in the panel sheeting is the sum of Eqs. (16) and (18)

$$U^k = \frac{1}{2}(\frac{b\alpha_1}{Gwt} + \frac{144h^3\ell^2\alpha_2}{Et^3wbd}) Q^2 \tag{20}$$

By equating the strain energy in the work done by the shear force 1/2 $Qb\gamma^k$, it can be seen that

$$Q = \frac{b\gamma^k}{f} \tag{21}$$

in which f denotes the bracketed term of Eq. (20). Substitution of Eq. (21) into Eq. (20) results in the expression for the strain energy in terms of the generalized shear deformation γ:

$$U^k = \frac{1}{2} s^k \gamma^k \gamma^k \tag{22}$$

in which

$$s^k = \frac{b^2}{f} \tag{23}$$

Cladding stiffness matrix -- The total strain energy in the cladding is found by summing up the contributions of the fasteners and of the panels. This process leads to the assembly of the diaphragm stiffness matrix [S], which, in effect, can be directly obtained by adding the matrices of Eqs. (11), (14) and (23) in accordance with the corresponding degrees of freedom. The resulting matrix has the form

$$[S]_{4n+1\times 4n+1} = \begin{bmatrix} [S_{rr}]_{1\times 1} & [S_{ri}]_{1\times 4n} \\ [S_{ir}]_{4n\times 1} & [S_{ii}]_{4n\times 4n} \end{bmatrix} \tag{24}$$

in which the subscripts r and i denote, respectively, the "exterior" degree of freedom, r, and the interior ones:

$$\langle u^1 \; v^1 \; \theta^1 \; \gamma^1 \; \ldots \; u^n \; v^n \; \theta^n \; \gamma^n \rangle \tag{25}$$

By applying a static condensation procedure to eliminate the interior degrees of freedom in Eq.(24), the stiffness equation of Eq. (3) becomes

$$S^*_{rr} \; r = P \tag{26}$$

in which S^*_{rr} is the reduced stiffness matrix of order 1 by 1 and can be recognized as the "conventional" diaphragm stiffness. The process of static condensation can be conveniently carried out with the computer program described in Ref. (12).

The stiffness S^*_{rr} so determined does not take into account the flexibility of the perimeter members. The axial deformation in the horizontal perimeter members are neglected as these members are restrained by the frame girders. The strain energy in the two vertical perimeter members is (Fig.5a)

$$U_a = \frac{1}{2}\left(\frac{2}{3}\frac{b^3}{EAa^2}\right) P^2 \tag{27}$$

in which A = cross-sectional area of a vertical perimeter member. Eq.(27), when combined with the strain energy due to all the other factors, $\frac{1}{2}\frac{P^2}{S^*_{rr}}$, leads to a modified expression for the diaphragm stiffness

$$S^m_{rr} = \left[\frac{1}{S^*_{rr}} + \frac{2}{3}\frac{b^3}{EAa^2}\right]^{-1} \tag{28}$$

STIFFNESS MATRIX OF INTEGRATED STRUCTURE

The connections between the diaphragm perimeter members and the frame members are assumed capable of sustaining the forces F_1 to F_4 shown in Fig. 5(b). Let [T] be the transformation matrix defined by

$$[T]^T = \langle 1 \quad -1 \quad -\frac{b}{a} \quad \frac{b}{a} \rangle \tag{29}$$

such that

$$\{F\} = [T]P \tag{30}$$

By applying the contragradient law of transformation, the diaphragm stiffness matrix, incorporating the three rigid body motions of the diaphragm can be shown to be (the degrees of freedom are 1 to 4 in Fig. 5(b))

$$[k] = [T]S^m_{rr}\,[T]^T$$

i.e.

$$[K] = \begin{bmatrix} 1 & -1 & -\frac{b}{a} & \frac{b}{a} \\ & 1 & \frac{b}{a} & -\frac{b}{a} \\ \text{Sym.} & & \frac{b^2}{a^2} & -\frac{b^2}{a^2} \\ & & & \frac{b^2}{a^2} \end{bmatrix} S^m_{rr} \tag{31}$$

It can be seen from the above expression that the lateral displacements (coordinates 1 and 2) can affect the column axial forces (coordinates 3 and 4).

The above diaphragm stiffness matrix can be directly added to the stiffness matrix of the bare frame in accordance with the direct stiffness method. This procedure does require some modifications of existing computer programs for frame analysis. However, if column axial deformations can be neglected, the analysis of the integrated structure could be carried out by conventional frame programs as explained below. Ignoring the last two columns and rows of the matrix [k] in Eq.(31), the diaphragm matrix becomes

$$[k] = S^m_{rr} \begin{bmatrix} 1 & -1 \\ -1 & 1 \end{bmatrix} \qquad (32)$$

The above matrix is identical to the stiffness matrix of a truss member or a spring of stiffness S^m_{rr}. Thus, a diaphragm between two levels can be modelled by a horizontal spring attached to the upper level with the lateral displacement of the loose end of the spring coupled to that of the lower level. The use of this artifice necessitates the knowledge of the diaphragm stiffness S^m_{rr}, which can be evaluated using the existing simplified methods (2,13); and the results obtained would be identical to those from Dakhakhni's flexibility method (9) in the case of static loading.

RESPONSE OF CLAD FRAMES

To verify the validity of the cladding stiffness matrix presented, the two diaphragms tested by Nilson (14) are considered.

Diaphragm No.57-2 has the dimensiona a = 12 ft.(3.66 m), and b = 10 ft.(3.05 m) and consists of 6 panels of 16-gage continuous flat sheet stiffened by hat sections. The second diaphragm, designated by No.59-4, has 15 panels of 18-gage hat sections giving rise to the overall dimensions of a = 30 ft.(9.14 m) and b = 15 ft. (4.57 m). The welded connections are identical in both diaphragms. The end welds are 1 in.diameter (25.4 mm) puddle welds, 3 welds per panel end. The side welds are of similar size and spaced at 24 in.(61 cm) on centers. The seam welds are 1½ in. long (38.1 mm) at 18 in. (45.7 cm) on centers. The connection stiffnesses have been determined experimentally (15) at 1000 kips/in. (175 kN/mm) for the side weld; and 500 kips/in.

(87.6 kN/mm) for the seam weld.

Because of the presence of the continuous flat sheet, the factors α_1 and α_2 of Eq.(20) are set equal to 1 and 0 respectively. Thus, $f = 7.21 \times 10^{-3}$ in./kip(41.2×10^{-3} mm/kN) for diaphragm No.57-2, and $f = 13.5 \times 10^{-3}$ in./kip (77.1×10^{-3} mm/kN) for diaphragm 59-4. A summary of the spring forces, diaphragm stiffnesses and strengths is presented in Tables 1 and 2. In these tables, the tabulated fastener forces are the maximum values occurring in the end panels and are due to an applied load of 1 kip (4.45 kN). The results obtained by the present method are compared to those obtained by finite element analyses (15) and tests (14,15). It should be noted that the applied load in the diaphragm test No. 59-4 was in the direction parallel to the corrugation generator and thus, the tabulated theoretical values have already been transformed in accordance with the method described in Ref. (13). The values of the fastener forces and diaphragm flexibilities, by the present method, are generally lower than by the finite element analyses. This is understandable since the present model is overly stiff due to the use of only one degree of freedom for the entire perimeter frame. The diaphragm strengths are calculated based on the strength of the end-weld which was determined at 6.3 kips (28 kN) per weld (15). In practice, the possibility of buckling of the perimeter members and of the sheeting should also be investigated. Other applications of the present method to screw-connected roof diaphragms may be found in Ref.(16).

With regard to the response of the overall structures, two 3-bay clad frames are considered. The first frame has 26 stories, and the second one 40 stories with uniform cladding throughout the middle bay (Fig.6). Member sections change gradually along the height of the frames and are given Ref.(5). The two bare frames satisfy the strength requirements but fail to satisfy the lateral drift restrictions.

In previous studies (9,17) on the static response of multistory clad frames, it has been found convenient to characterise the responses of clad frames relative to those of the bare frames by means of the dimensionless ratio

$$\gamma = \frac{S^m_{rr}}{12 \, \Sigma \, \frac{EI_c}{L_c^3}} \qquad (33)$$

in which I_c, L_c = moment of inertia and length of the column; and the summation is carried out for all columns

in the story at a distance 5/6 of the building height from ground level. For the present application, a series of analyses corresponding to a range of values of γ was carried out. The masses of structural members and dead loads were input as lumped masses at the story levels. The National Building Code response spectra were used (18). Damping values of 3% and 5% were assumed for the bare and clad frames, respectively. Higher value of damping was used for the clad frames because of the high energy dissipation expected to occur in the cladding. However, for comparison purposes, additional analyses of the bare frame were carried out with 5% damping factor. The square root values of the sum of the squares of the first three modes were used to evaluate the frame responses.

In all cases, the results are expressed in dimensionless form as the ratio of the response in clad frame to that in the bare frame. Fig.7 shows the effects of cladding stiffness on the natural periods of the clad frame. As γ increases, the clad frame becomes stiffer and the period decreases. At $\gamma = 0.5$, the reduction is 20%, 25% and 29% in the 1st,2nd and 3rd mode respectively. With higher shear stiffness ratio, the reduction continues but less rapidly. The variation in the maximum drift of the frames is shown in Fig.8, where a reduction of 22% to 35% at $\gamma = 0.5$ can be obtained depending upon the damping value of the bare frame.

Figure 9 shows the variation of the maximum bending moments in columns and beams of the clad frame. It is observed that with 5% damping in both frames, the maximum bending moments in the members of clad frames are higher than those in the bare frames. However, with a more realistic value of 3% damping for the bare frames, these forces drop below the corresponding values in the bare frames. Generally, the maximum moments occur in the interior bottom column and in beams from the 2nd to the 5th floor. It should be noted that these maximum values sometimes do not occur in the same members of the bare and clad frames.

The ratio of the maximum shear in the cladding to the total story shear (cladding and columns) at the same level is plotted in Fig.10. Obviously, as the stiffness ratio increases, the cladding attracts more shear, but at a decreasing rate. The maximum shear often occurs at the 3rd story. Fig.11(a) shows the dramatic increase in the axial force of the interior bottom columns of the clad frames, especially for the 26-story frame. This is due to the reaction of the cladding on the interior columns. However, the large difference between the behaviour of the 40- and 26-story frames is unexpected. Apparently, this behaviour is related to the difference in the width of the

exterior bays of the two frames. In spite of this substantial increase in the interior column axial forces, the magnitude of this force is still less than that of the exterior column (Fig.12) for all values of γ in the case of the 40-story frame, and for $\gamma \leq 0.4$ in the case of the 26-story frame (see Fig.11(b) for variation of axial forces in exterior columns.)

An additional analysis of the 26-story frame with cladding in an exterior bay ($\gamma = 1$ and $\lambda = 5\%$) was performed. Compared to the corresponding values when cladding was placed in the middle bay, there was an increase of 8% in the maximum drift and a reduction of 9% in the sum of column axial forces of the bottom story.

CONCLUSIONS

Cold-formed steel cladding is effective for controlling the drift of multistory frames. In design, the shear stiffness and strength of cladding are important parameters, and special consideration should be given to the connection details between the cladding and the frame. A method for determining these design parameters has been presented and shown to be reliable. The integrated stiffness of both the frame and the cladding is obtained by means of a specially derived cladding stiffness matrix. The analysis of the overall structure is carried out using the conventional direct stiffness method. The technique is efficient in terms of computer storage and computation.

Earthquake response of two multistory clad frames has been presented in dimensionless form, which can be used to estimate the response of other clad buildings even though its validity still needs to be established by more extensive analyses. In general, light gage cladding with shear stiffness at 50% of the bare frame story stiffness may yield reduction up to 30% in deflection; however, member forces may also be increased. Overstiff cladding is not recommended since it attracts large shear load and tends to increase dramatically the axial forces in the adjacent columns. Further study on the energy dissipation capacity as well as the overall ductility of cladding is required before structural cladding can be used with confidence.

REFERENCES

1. Design of Light-Gage Steel Diaphragms, American Iron and Steel Institute, New York, N.Y., 1967.

2. European Recommendations for Stressed Skin Design of Steel Structures, published by ECCS (Committee 17), Salford, England, 1977.

3. Davies, J.M., "A Bibliography on the Stressed Skin Action of Light Gauge Steel Cladding", University of Salford, Dept. of Civil Engineering, Report No. 75/63, 1975.

4. Miller, C.J., "Analysis of Multi-Storey Frames With Light-Gauge Steel Panel Infills", thesis presented to Cornell University, at Ithaca, N.Y., in 1972, in partial fulfillment of the requirements for the degree of Doctor of Philosophy.

5. Miller, C.J., and Serag, A.E., "Dynamic Response of Infilled Multistory Steel Frames", Fourth International Specialty Conference on Cold-Formed Steel Structures, Vol.II, University of Missouri-Rolla, 1978, pp.557-586.

6. Oppenheim, I.J., "Control of Lateral Deflection in Planar Frames Using Structural Partitions", Proceedings of the Institute of Civil Engineers, London, England, Vol.55, June, 1973.

7. Oppenheim, I.J., "Dynamic Behavior of Tall Building With Cladding", Proceedings of the Fifth Conference on Earthquake Engineering, Rome, 1973, pp.2769-2773.

8. Bryan, E.R. and Davies, J.M., "Diaphragm Action in Multistory Buildings", University of Salford, Dept.of Civil Engineering, Report No.75/70, Jan., 1976.

9. El-Dakhakhni, W.M., "Effect of Light-Gage Partitions on Multi-story Buildings", Journal of the Structural Division, ASCE, Vol.103, No.ST1, Proc. Paper 12672, Jan., 1977, pp.119-132.

10. Bryan, E.R. and El-Dakhakhni, W.M., "Shear Flexibility and Strength of Corrugated Decks", Journal of the Structural Division, ASCE, Vol.94, No.ST11, Proc. Paper 6218, Nov., 1968, pp.2549-2580.

11. Davies, J.M. and Lawson, R.M., "The Shear Deformation of Profiled Metal Sheeting", International Journal for Numerical Methods in Engineering, Vol. 12, 1978, pp.1507-1541.

12. Ha, H.K., "A Multi-Purpose Gauss Routine For Unbanded Symmetric Matrix", to appear in International Journal for Numerical Methods in Engineering, 1979.

13. Ha, H.K., El-Hakim, N., and Fazio, P., "Refined Calculations of Strengths and Stiffnesses of Cold-Formed Steel Diaphragms, To Appear in Canadian Journal of Civil Engineering, June 1979.

14. Nilson, A.H., "Shear Diaphragms of Light-Gauge Steel", Journal of the Structural Division, ASCE, Vol. 86, No. ST11, Proc. Paper 2650, Nov., 1960, pp.111-139.

15. Ammar, A.R. and Nilson, A.H., "Analysis of Light Gauge Steel Shear Diaphragms", Research Report No. 351, Cornell University, Ithaca, N.Y., Apr., 1973.

16. Ha, H.K., "Analysis of Corrugated Shear Diaphragms", Journal of the Structural Division, ASCE, Vol.105, No.ST3, March, 1979.

17. Ha, H.K., "Lateral-Load Behavior of Multistory Frames Stiffened With Corrugated Panels," Symposium on Behavior of Building Systems and Building Components, Vanderbilt University, March 8-9, 1979.

18. Supplement No. 4 to the National Building Code of Canada, National Research Council of Canada, Ottawa, 1977.

TABLE 1 - Summary of Results for Diaphragm 57-2

Data	Present Method	Finite Element Analysis [1]	Experimental [1]
Number of degrees of freedom used	25	858	-
Side Fastener force, in pounds	114.	135.	-
Seam Fastener force, in pounds	92.	104.	-
Maximum end fastener force, in pounds	151.	171.	-
Stiffness, in kips/inch	330.	305.	303.
Strength, in kips	41.5	36.8	38.6

Note: 1 lb. = 4.45 N; 1 in. = 25.4 mm

TABLE 2 - Summary of Results for Diaphragm 59-4

Data	Present Method	Finite Element Analysis [1]	Experimental [1]
Number of degrees of freedom used	61	1230	-
Side Fastener force, in pounds	97.	104.	-
Seam Fastener force, in pounds	89.	95.	-
Maximum end fastener force, in pounds	126.	145.	-
Stiffness, in kips/inch	114.	100.	114.
Strength, in kips	49.8	43.5	47.8

Note: 1 lb. = 4.45 kN; 1 in. = 25.4 mm

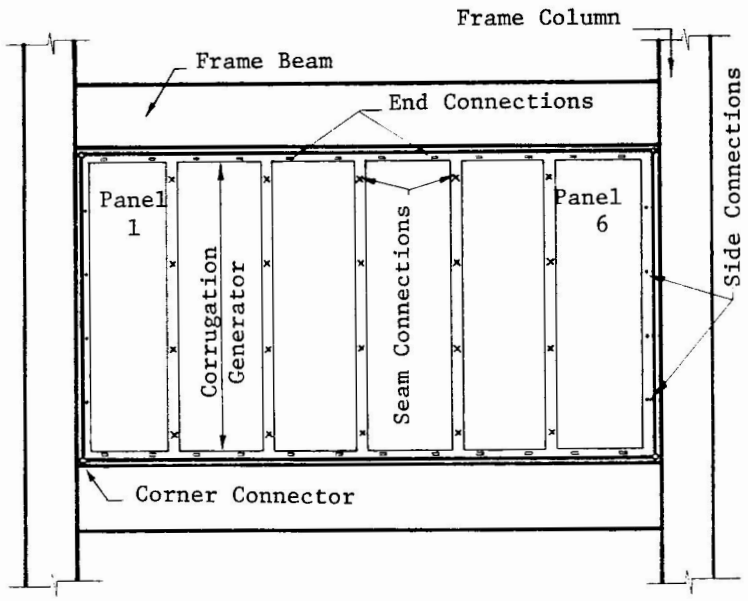

FIG. 1 - COMPONENTS OF CLADDING

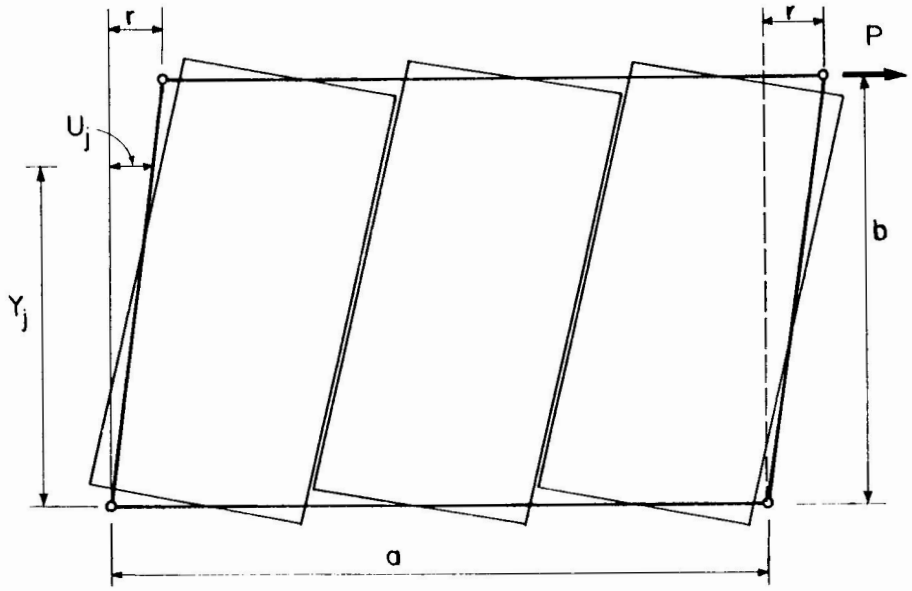

FIG. 2 - DEFORMATION MODE OF CLADDING

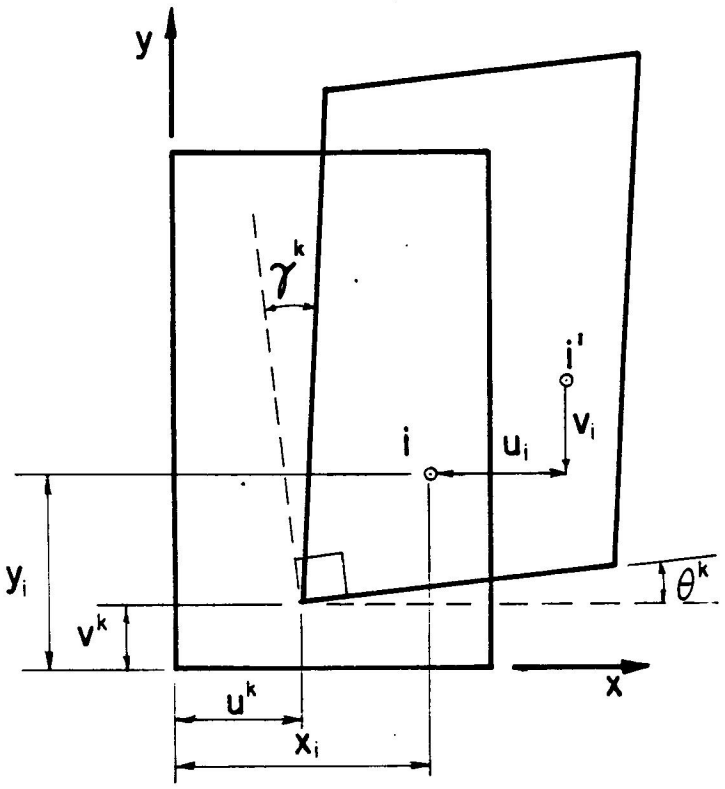

FIG. 3 - PANEL DEGREES OF FREEDOM

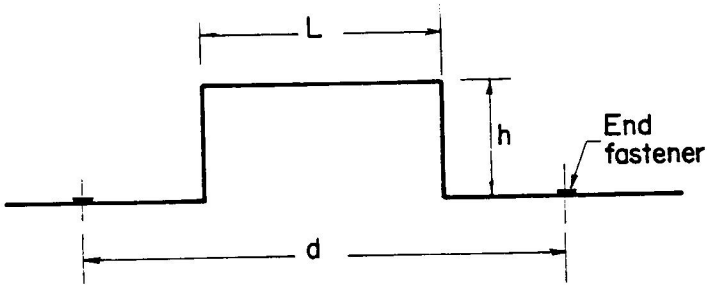

FIG. 4 - OPEN RECTANGULAR PROFILE

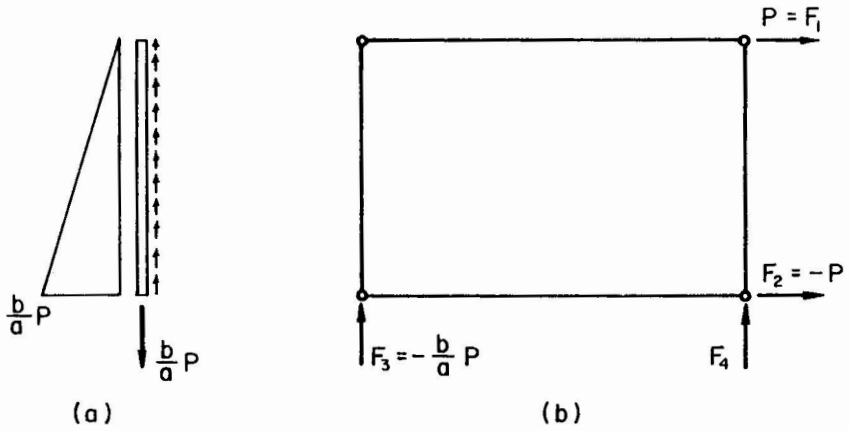

FIG. 5 - (a) AXIAL FORCE DISTRIBUTION IN VERTICAL PERIMETER MEMBERS; (b) COORDINATES OF CLADDING

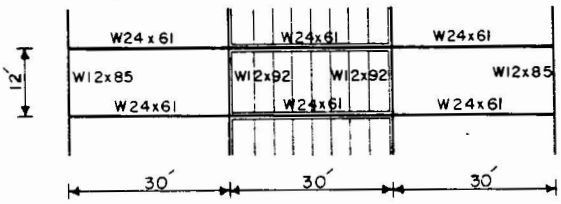

a) 22nd story of 26 story frame

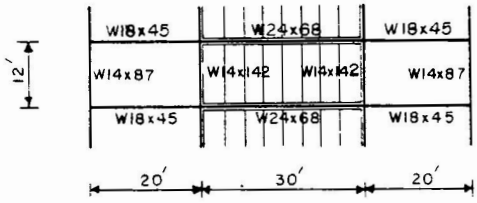

b) 34th story of 40 story frame

FIG. 6 - SEGMENTS OF EXAMPLE FRAMES

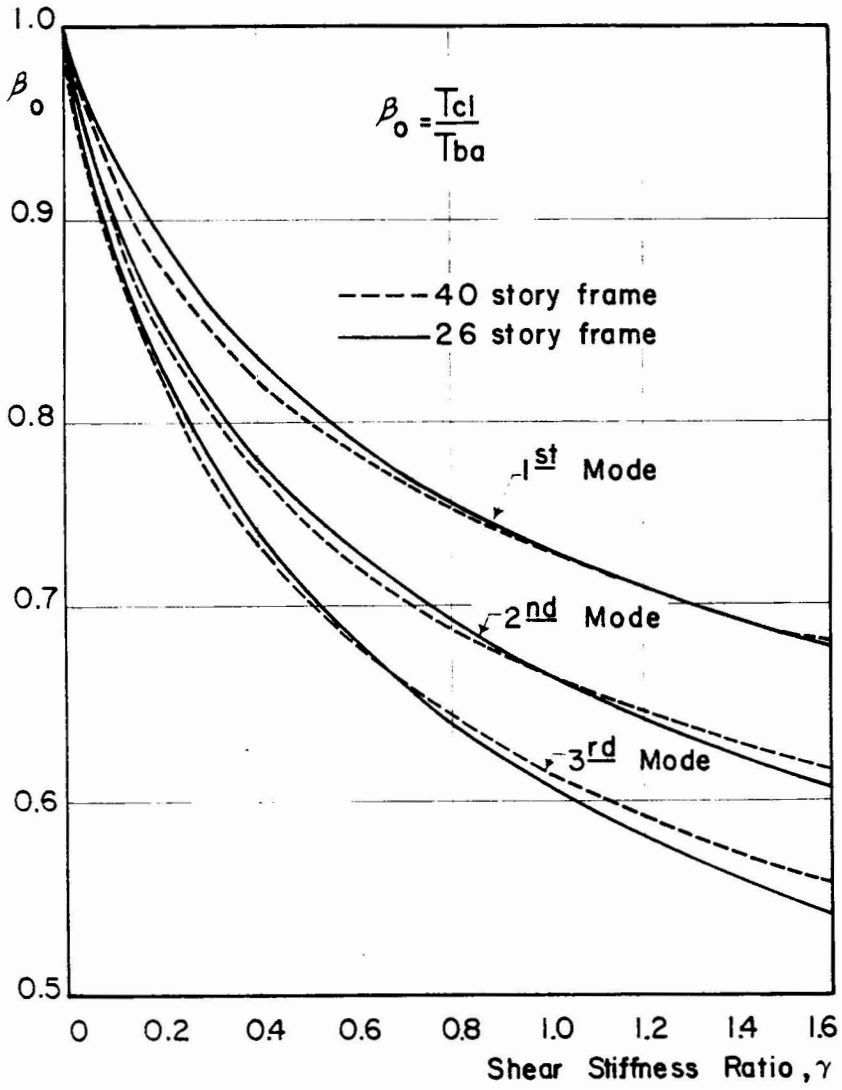

FIG. 7 - VARIATION OF THE NATURAL PERIOD

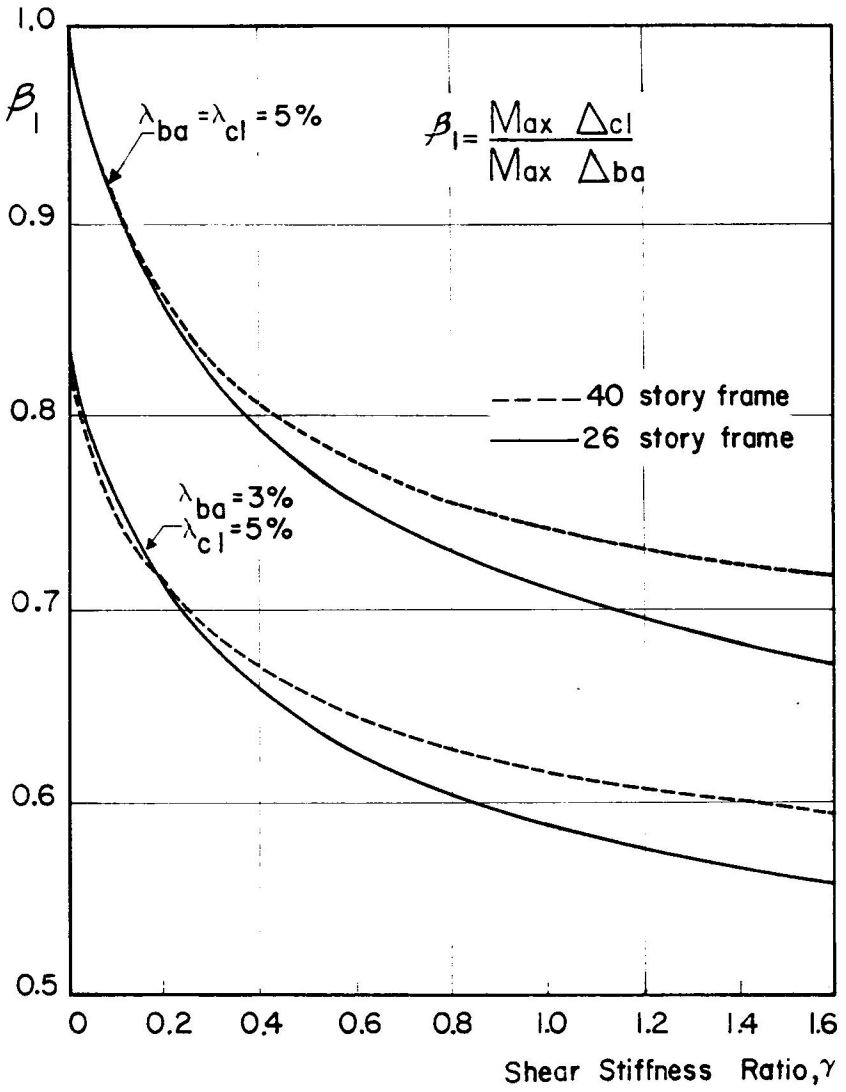

FIG. 8 - VARIATION OF MAXIMUM DRIFT

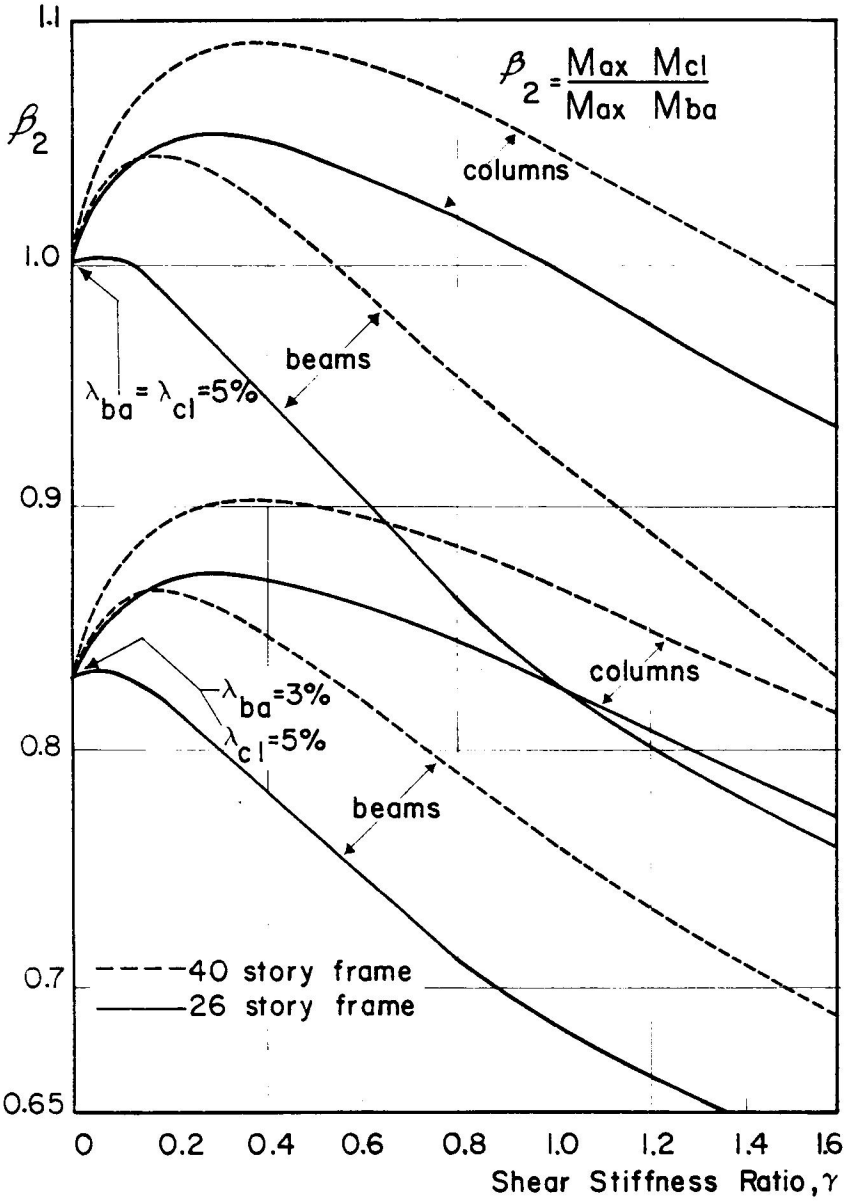

FIG. 9 - VARIATION OF MAXIMUM BENDING MOMENTS

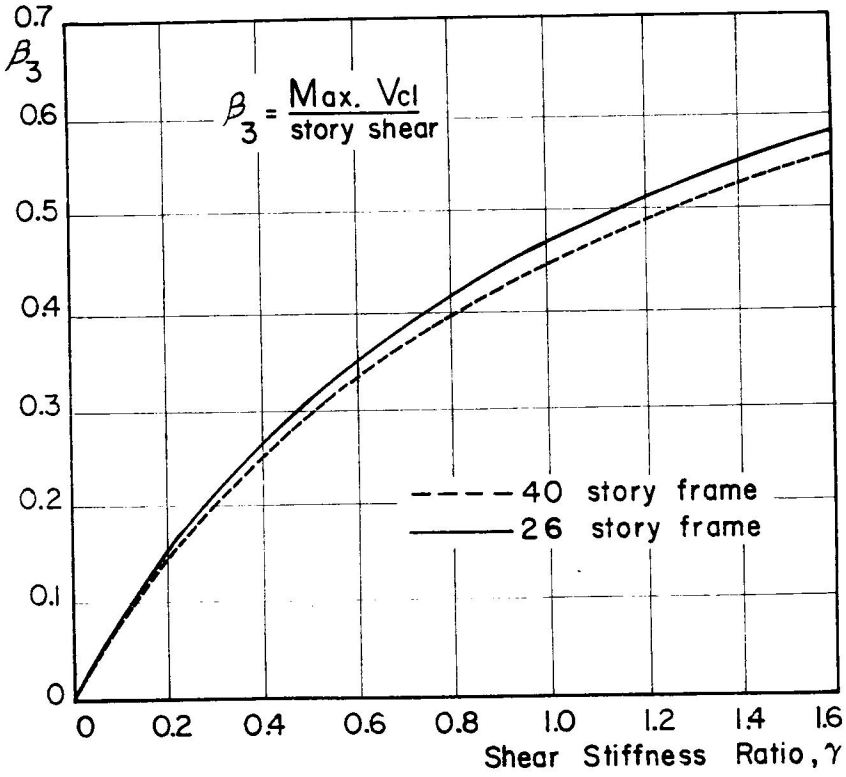

FIG. 10 - VARIATION OF MAXIMUM SHEAR FORCE IN CLADDING

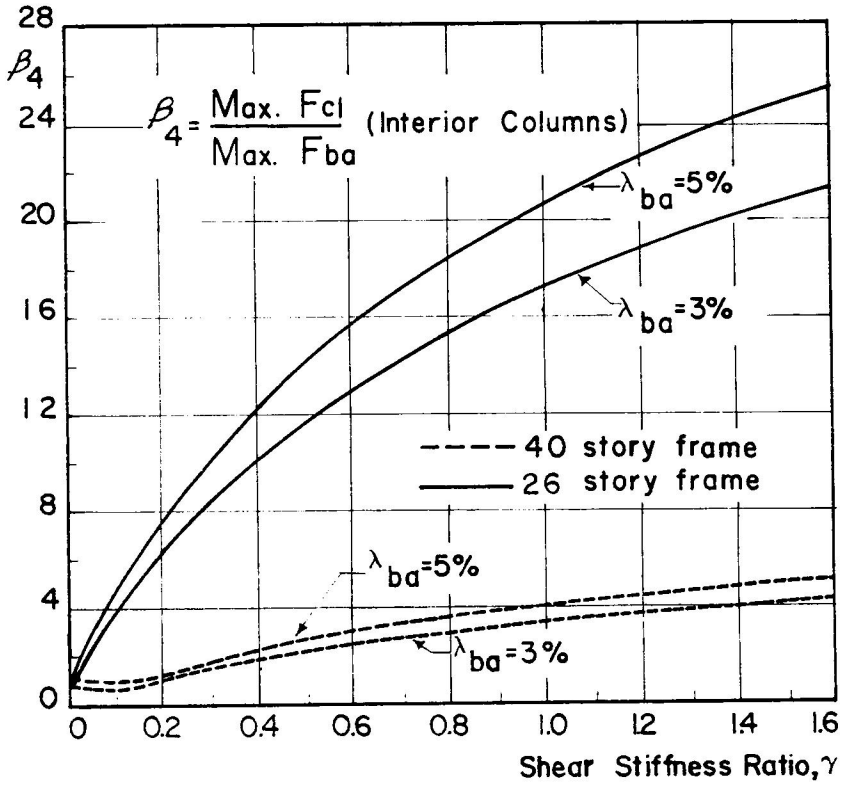

FIG. 11a - VARIATION OF MAXIMUM AXIAL FORCES IN THE INTERIOR COLUMNS

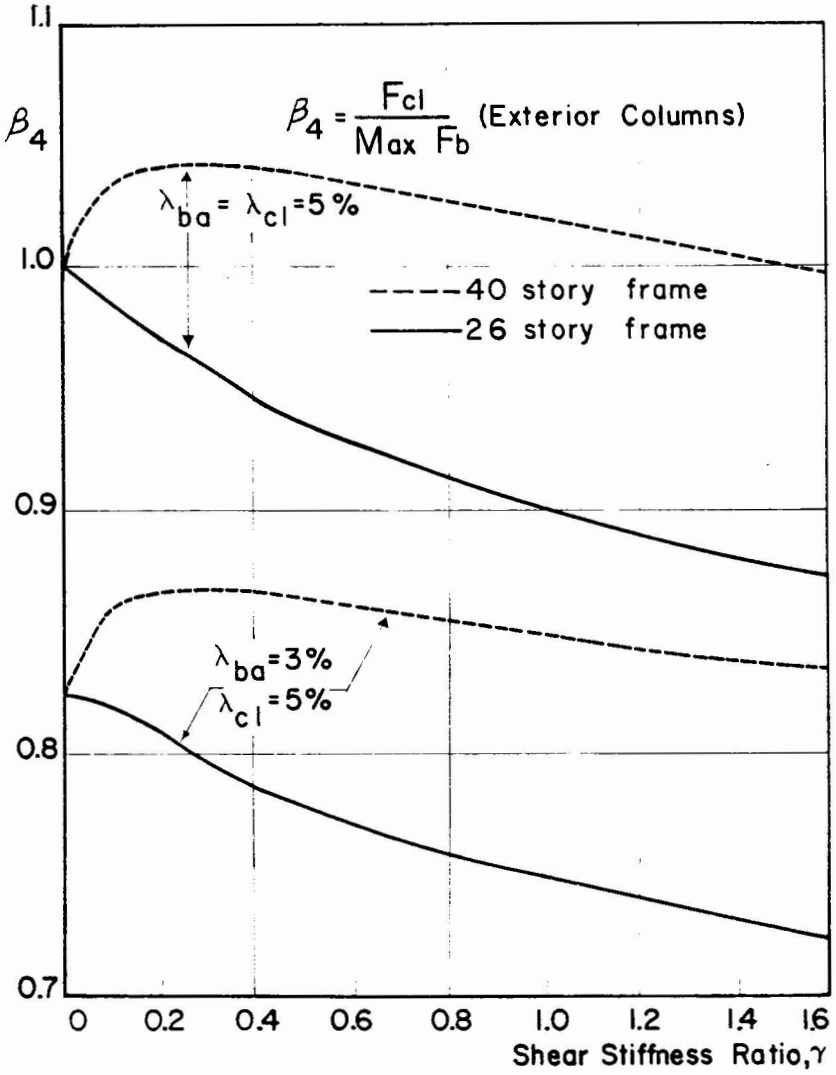

FIG. 11b - VARIATION OF MAXIMUM AXIAL FORCES IN EXTERIOR COLUMNS

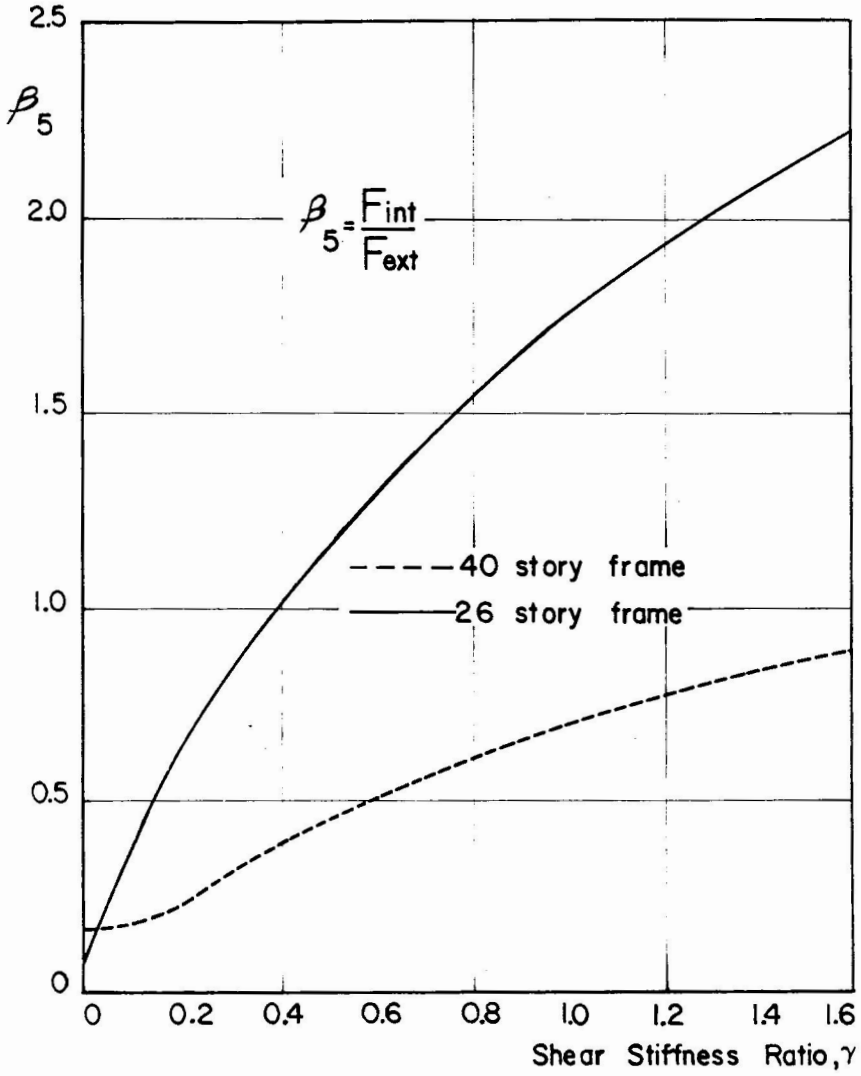

FIG. 12 - VARIATION OF THE RATIO OF THE MAXIMUM AXIAL FORCES IN INTERIOR TO EXTERIOR COLUMNS